

# Two-Fluid Behaviour at the Origin of the Resistivity Peak in Doped Manganites

D. I. Golosov, N. Ossi, and A. Frydman

*Department of Physics and the Resnick Institute, Bar-Ilan University, Ramat-Gan 52900, Israel*

I. Felner, I. Nowik, and M. I. Tsindlekht

*Racah Institute of Physics, The Hebrew University, Jerusalem 91904, Israel*

Y. M. Mukovskii

*Moscow State Steel and Alloys Institute, 119049 Moscow, Russia*

(Dated: February 20, 2019)

We report a series of magnetic and transport measurements on high-quality single crystal manganese samples in the colossal magnetoresistive regime. 1 % Fe doping allows Mössbauer spectroscopy study, which shows (i) unusual line broadening within the ferromagnetic phase and (ii) a coexistence of ferro- and paramagnetic contributions around the Curie point  $T_C$ . For some of our samples, the resistivity peak occurs at a considerably higher temperature,  $T_{MI}$ . This shows that phase separation into metallic (ferromagnetic) and insulating (paramagnetic) phases cannot be generally responsible for the resistivity peak (and hence for the associated colossal magnetoresistance). In addition, our data imply that the transitions at  $T_C$  and  $T_{MI}$  are two distinct phenomena on their own right, with distinct (although probably interrelated) physical origins. We speculate that these results can be understood phenomenologically within the two-fluid approach.

PACS numbers: 75.47.Gk, 75.47.Lx, 76.80.+y

The phenomenon of colossal magnetoresistance (CMR) in doped manganese oxides continues to attract extensive research effort[1]. While the physical mechanism underlying the CMR phenomenon remains elusive, one can expect it to be generic for the entire family of the CMR compounds, spanning a broad range of chemical compositions, dopant levels, and lattice properties. This natural suggestion is corroborated by the fact that, in addition to the CMR itself, other generic unusual features of the CMR compounds have been found in recent years. These include the formation of a “pseudogap” in the carrier density of states on increasing temperature toward  $T_C$  [2] (arguably responsible for the peak in the resistivity,  $\rho(T)$ , which in turn gives rise to the CMR effect), and the unusual short-range magnetic correlations in the critical region (“central peak”), observed in the neutron scattering experiments[3]. Although these findings testify to the anomalous electronic and magnetic properties respectively, the relationship between the two remains unclear. While it is generally understood that the metal-insulator transition (at  $T_{MI}$ , corresponding to the resistivity peak) and the ferro- to paramagnetic transition (at the Curie temperature  $T_C$ ) lie close to each other, the consensus does not go much further. Indeed, questions relating to the mutual location of the two transitions[4, 5] (whether  $T_C$  actually *equals*  $T_{MI}$ ), as well as to their character, remain largely open. This situation is partly due to sample preparation issues, which make it difficult to draw a quantitative connexion between results of different measurements, carried out on different samples.

On the theory side, the picture is similarly uncertain. Current ideas on the mechanism of the CMR mainly fall within two general categories, which can be re-

ferred to phenomenologically without specifying the microscopic models or even the relevant degrees of freedom. The first one is the so-called *phase separation scenario*[6, 7], whereby the metallic (ferromagnetic) and insulating (paramagnetic) phases coexist in the temperature region around  $T_C$ . With decreasing temperature, the volume fraction of ferromagnetic “droplets” grows, resulting in an eventual percolation and metallic behaviour at low  $T$ . The long-range ferromagnetic order is also linked to connectivity between the ferromagnetic clusters and is established at about the same point.

The second theoretical view is that of the *two-fluid model*[8], based on the coexistence[9] of (i) localised carriers (or polarons [10]) and (ii) itinerant conduction electrons below  $T_{MI}$ , in a spatially homogeneous (on a sub-micron scale) system. While the high-temperature insulating properties are accounted for by the fact that all carriers are localised, lowering the temperature leads to an increase of the itinerant carrier population. This in turn results in (i) the resistivity passing through a maximum and decreasing towards lower  $T$  and (ii) strengthening the ferromagnetic interaction in the system via the double exchange mechanism[11], which is more effective for the itinerant electrons than for the localised ones[12]. In principle, the ferromagnetic order can be established above or below the downturn of the resistivity. Thus, while the physics behind the magnetic transition at  $T_C$  can be that of thermal fluctuations overpowering the ferromagnetism, the electronic transition at  $T_{MI}$  is due to a (presumably strongly correlated) mechanism leading to the disappearance of itinerant carriers at higher  $T$ .

In the present letter, we report a series of magnetic and transport measurements. All of these were performed on

the *same* high-quality manganite single crystals. Our findings appear incompatible with the percolative nature of the metal-insulator transition (as in the phase separation scenario). They also imply that the ferro- to paramagnetic and electronic (metal-insulator) transitions are two distinct phenomena with no rigid interconnection. Indeed, the metal-insulator transition at  $T_{MI} \neq T_C$  leads to a change of the Curie-Weiss temperature and therefore to a separate feature in the *magnetic* properties of the system at  $T = T_{MI}$ . These results can be understood in the framework of the two-fluid approach.

While the two compounds,  $\text{Pr}_{1-x}\text{Sr}_x\text{MnO}_3$  (PSMO) and  $\text{La}_{1-x}\text{Ca}_x\text{MnO}_3$  (LCMO) with  $0.2 \lesssim x \lesssim 0.5$  show metallic behaviour at low  $T$  and CMR near  $T_C$ , their properties differ significantly. The unconventional magnetic behaviour (giving rise to the central peak as observed near  $T_C$  in the neutron scattering experiments[3]), first found in LCMO, is much less pronounced in the PSMO[3]. The neutron scattering central peak originates from unusual short-range magnetic correlations, which should also be accessible via a local (i.e., momentum-integrated) magnetic probe, such as Mössbauer spectroscopy of iron-doped samples. Earlier Mössbauer studies of the CMR manganites[13, 14, 15] indeed uncovered an unusual coexistence of para- and ferromagnetic contributions to the hyperfine field near  $T_C$ [16].

Single crystals of pure and  $^{57}\text{Fe}$ -doped PSMO and LCMO (with  $x = 0.3$ ) were grown by non-crucible floating-zone melting with radiation heating[17]. X-ray diffraction and EPMA (Electron Probe Micro Analysis) measurements were performed to verify that the samples are single phase crystals of the nominal compositions. Properties of the samples are summarised in Table I. As expected[18], the 1% substitution of Mn by enriched  $^{57}\text{Fe}$  (needed for Mössbauer spectroscopy) in the two PSMO-F [19] and LCMO-F samples does not significantly change the respective system properties.

Magnetisation measurements were performed in a commercial (Quantum Design) SQUID magnetometer. The in-phase component of the zero-field ac susceptibility (measured at 1065 Hz, amplitude 0.05 Oe) and the standard four contact resistivity were measured by homemade probes inserted into the magnetometer. Pieces of LCMO-F and PSMO-F crystals were crushed to powder for the Mössbauer measurements. These were performed using a constant acceleration drive in transmission mode and a 50 mCi  $^{57}\text{Co} : \text{Rh}$  source. Measurements taken at liquid Helium temperature revealed well-defined sextet spectra (not shown), indicating that the Fe ions were located at a specific lattice site (presumably that of Mn). Further measurements were performed between 90K and 300 K, and the obtained spectra were fitted to simulated models.

Our Mössbauer results are represented in Figs. 1 and 2. Fig. 1 shows a sequence of Mössbauer spectra for the LCMO-F sample. While the spectra at 90 K and 230 K show the magnetically ordered (sextet) and paramagnetic

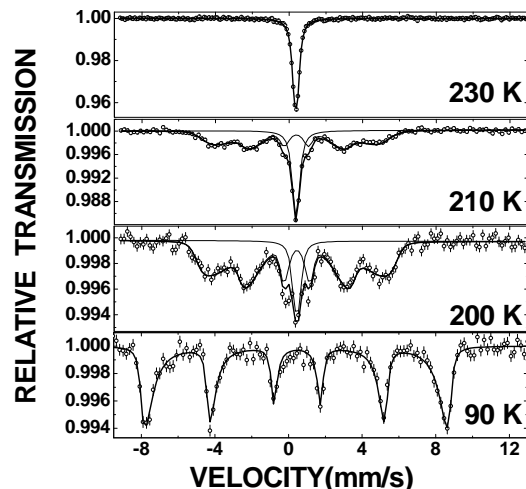


FIG. 1: A selection of the LCMO-F spectra at various temperatures. Solid lines represent the simulated sub-spectra; notice the coexistence of ferro- and paramagnetic contributions at 200K and 210 K.

(singlet) behaviour respectively, a superposition of the two contributions is clearly observed between  $T_1 \approx 190\text{K}$  and  $T_2 \approx 230\text{K}$  (cf. Fig. 2). Above  $T_1$ , both the relative intensity of the ferromagnetic component (fraction of magnetically ordered sites, Fig. 2, shown also for PSMO-F) and the value of the hyperfine field characterising the ferromagnetic contribution decrease and ultimately vanish at  $T_2$ . The long-range magnetic order, on the other hand, disappears at  $T_C = 224\text{K}$ [20],  $T_1 < T_C < T_2$ .

We find that for PSMO-F the ferromagnetic fraction disappears more abruptly (mostly at  $210\text{K} < T < 230\text{K}$ , see Fig. 2, top panel), in agreement with the more conventional critical properties found by neutron scattering[3]. Note that the increase of resistivity  $\rho$  with  $T$  (for  $T \lesssim T_{MI}$ ) is steeper in the case of LCMO-F (Figs. 2 and 3). Phase separation scenario would imply the opposite trend.

Our low- $T$  resistivity data are best fitted by[21]  $\rho = \rho_0 + \rho_1 T^{5/2}$ . With increasing temperature,  $\rho(T)$  passes through a maximum at  $T = T_{MI}$ , followed by an activated-type dependence,  $\rho \sim \exp(\Delta/k_B T)$  with  $\Delta \sim 0.07\text{ eV}$  at higher  $T$ . In the case of PSMO-F, magnetically ordered sites are absent already at  $T_2 = 230\text{K}$ , some 15 K below  $T_{MI}$ . This is similar to earlier results for  $\text{La}_{0.8}\text{Ca}_{0.2}\text{MnO}_3$  (with  $T_{MI} - T_2 \approx 7\text{K}$ )[14]. *Such behaviour is impossible to reconcile with the phase separation scenario*, which implies that the disappearance of metallic ferromagnetic areas occurs *above*  $T_{MI}$ . Indeed, the effective-medium calculation[22] for resistivity at a given value of metallic fraction suggests that  $T_{MI}$  is well below the actual value (Figs. 2 and 3).

In the case of LCMO-F, Mössbauer spectra at 230 K (only slightly below  $T_{MI}$ ) still indicate some presence of magnetically ordered sites [ $1(\pm 1)\%$  fraction]. The resistivity data are in a perfect agreement with the effec-

TABLE I: Samples – compositions and measured properties, including: Curie and paramagnetic Curie–Weiss temperatures,  $T_C$  and  $T_{CW}$  (from magnetic measurements); metal-insulator transition temperature,  $T_{MI}$  and transport gap  $\Delta$ , from the transport experiments. Coexistence of ferro- and paramagnetic contributions to Mössbauer spectra takes place at  $T_1 < T < T_2$ .

Sample	Composition	$T_1$ , K	$T_2$ , K	$T_C$ , K	$T_{MI}$ , K	$\Delta$ , eV	$T_{CW}$ , K
PSMO	$\text{Pr}_{0.7}\text{Sr}_{0.3}\text{MnO}_3$			218	245	0.068	205
PSMO-F	$\text{Pr}_{0.7}\text{Sr}_{0.3}\text{Mn}_{0.99}\text{Fe}_{0.01}\text{O}_3$	180	230	223	244	0.064	221
LCMO-F	$\text{La}_{0.7}\text{Ca}_{0.3}\text{Mn}_{0.99}\text{Fe}_{0.01}\text{O}_3$	190	230	224	231	0.078	221

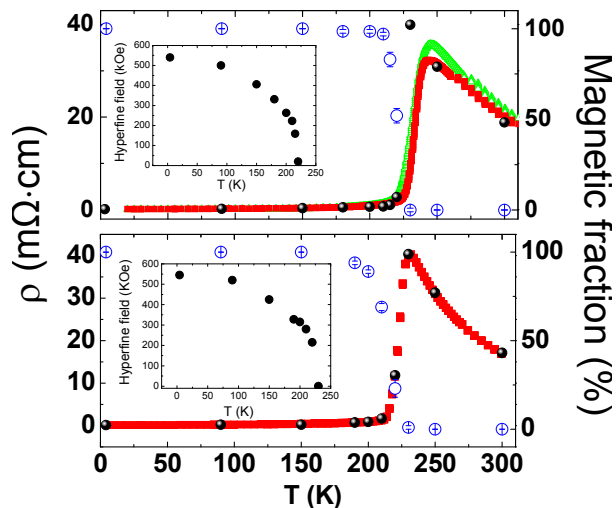


FIG. 2: (colour online) Mössbauer and transport data. Magnetically ordered fraction (open circles with error bars, right scale) and resistivity  $\rho(T)$  (filled squares, left scale) for the PSMO-F (top) and LCMO-F (bottom) samples. Triangles (top) show  $\rho(T)$  for the pure PSMO sample. Bullets correspond to the effective-medium[22] values of  $\rho(T)$  for PSMO-F and LCMO-F. Temperature dependences of magnetic hyperfine fields are plotted in the insets.

tive medium description. This is in line with earlier results[15] for  $\text{La}_{0.67}\text{Ca}_{0.33}\text{Mn}_{0.99}\text{Sn}_{0.01}\text{O}_3$ . Note however that one expects the origins of the resistivity peak to be the same in all cases. Therefore *the apparent success of phase-separation scenario in describing LCMO-F should be viewed as incidental*, stemming from the relatively low value of  $T_{MI} - T_C$  for this case (Table I). It is also possible that the (nearly) first-order transition[3, 23] observed in LCMO (with  $x \geq 0.3$ ) at  $T_C$  is accompanied by phase separation and circumvents a more generic behaviour, thereby masking the physics behind the resistivity peak.

An alternative interpretation is provided by the two-fluid approach, which allows for the itinerant electrons in the paramagnetic phase. On the other hand, continued presence of localised electrons below  $T_2$  may explain the origin of the paramagnetic contribution to the Mössbauer spectra. Between the sites where the wave function of a localised electron is centred, the ferromagnetic double exchange coupling is weaker than elsewhere[12], hence the

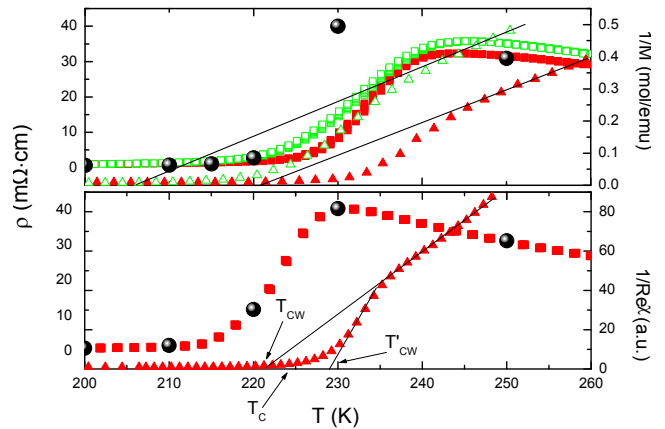


FIG. 3: (colour online) Filled triangles show the inverse low-field (10-20 Oe) magnetisation  $1/M$  for PSMO-F (top) and inverse ac susceptibility  $1/\text{Re}\chi$  for LCMO-F (bottom). Filled squares represent corresponding values of  $\rho(T)$ , whereas bullets are the effective medium result for  $\rho$ . Open symbols (top) show  $1/M$  and  $\rho$  for PSMO; lines are guide to the eye.

corresponding spins order at a lower  $T < T_2$ . Even below  $T_1$ , when uniform ferromagnetic order is maintained, thermal fluctuations of these spins will be stronger, corresponding to a broad distribution of the hyperfine field values. Indeed, we observe an asymmetric line broadening in the Mössbauer spectra of both LCMO-F and PSMO-F at  $90\text{K} < T < T_2$  (with linewidths, for  $T > 150\text{K}$ , reaching over 50% of the hyperfine field value). We note that the earlier Mössbauer studies[13, 14, 15], carried out typically on ceramic samples (which are expected to be less homogeneous than single crystals)[24], suggested the coexistence of ferro- and paramagnetic contributions down to lower  $T$ , and/or the presence of several distinct ferro- (at low  $T$ ) or paramagnetic (at high  $T$ ) phases. The continuous hyperfine field distribution observed in our samples is, on the other hand, most probably due to either the continuous (static) distribution of ferromagnetic interaction strengths (due to the presence of localised electrons) or to spin fluctuations in a single ordered phase, with the fluctuation rate comparable to the nuclear magnetic Larmor frequency[25].

We next turn to the temperature dependence of the inverse magnetisation (shown in Fig. 3 for PSMO and

PSMO-F) and notice that it deviates downward from the Curie–Weiss law,  $H/M \propto T - T_{CW}$ , when approaching  $T_C$  from the paramagnetic side (cf. “magnetisation kink” [9]). In all cases, the inverse ac susceptibility shows the same feature (see Fig. 3, bottom panel). This deviation starts at a point which can be recognised as the metal-insulator transition temperature,  $T_{MI}$  (within 2-3K accuracy). We emphasise that this (and *not* the Curie ferro-to paramagnetic transition!) is a manifestation of the resistivity peak in the *magnetic* properties of the system.

In the literature[22], the downturn of  $1/M(T)$  is often identified as a Griffiths singularity (denoted  $T_G$ ). It implies that at  $T_C < T < T_G$ , the inhomogeneity of effective exchange couplings gives rise to (fluctuating) ferromagnetic metallic clusters, resulting in the resistivity downturn at  $T = T_{MI} < T_G$ . We note that one does expect an inhomogeneity of exchanges in a system where localisation of the conduction electrons leads to an inhomogeneous charge distribution; this probably accounts for the deviation of  $1/M$  from the high-temperature Curie–Weiss law, characterised by  $T_{CW}^\infty > T_{CW}$ . This deviation, however, occurs at much higher temperatures,  $T/T_C \sim 1.5-2$  [26]. As for the ferromagnetic cluster formation, our results as outlined above allow for this only below the temperature  $T_2$ , which in the case of PSMO-F is well below  $T_{MI}$  (see Table I). The Griffiths phase approach may thus prove relevant for the analysis of magnetic critical properties of the manganites near  $T_C$ , but *not* for understanding the origins of the resistivity peak at  $T = T_{MI}$ .

This behaviour of  $1/M(T)$  is, on the other hand, easy to understand within the two-fluid approach. The itinerant carriers, which would appear once the temperature approaches  $T_{MI}$  from above, strengthen the double-exchange ferromagnetism[12]. This gives rise to the increase of  $T_{CW}$ [27] below  $T_{MI}$ ; we note that our plots of  $1/M(T)$  suggest possible presence at  $T_C < T < T_{MI}$  of an intermediate Curie–Weiss behaviour,  $1/M \propto T - T'_{CW}$  (with  $T'_{CW}$  slightly larger than  $T_C$ , as expected for a Curie–Weiss temperature in a conventional magnet). While the abrupt change of  $T_{CW}$  at  $T = T_{MI}$  would suggest the first-order nature of the metal-insulator transition, we leave this question for future study.

In conclusion, our results provide evidence against phase separation mechanism for the resistivity peak (and hence for the CMR phenomenon). On the other hand, we speculate that both the relationship between Mössbauer and transport data and the presence of two distinct transitions at  $T_C$  and  $T_{MI}$  (with the latter affecting also the magnetic properties) can be qualitatively understood within the two-fluid model.

We thank R. Berkovits, M. Golosovsky, L. Klein, E. M. Kogan, D. Orgad, V. Orlyanchik, O. A. Petrenko, and M. B. Salamon for illuminating discussions, and members of technical staff at our institutions for their valuable help. We acknowledge support of ISF 2004 Grant # 618/04, ISF 2005 Grant #249/05, and the Israeli Ab-

sorption Ministry.

- 
- [1] *Colossal Magnetoresistive Oxides*, Y. Tokura, ed. (Gordon and Breach, New York, 2000), and references therein.
  - [2] T. Saitoh *et al*, Phys. Rev. **B62**, 1039 (2000); D. S. Dessau and Z.-X. Shen, in Ref. [1]; Y.-D. Chuang *et al*, Science **292**, 1509 (2001); A. Biswas *et al* Phys. Rev. **B59**, 5368 (1999); J. Mitra *et al*, Phys. Rev. **B71**, 094426 (2005); note that optical [Y. Okimoto *et al*, Phys. Rev. Lett. **75**, 109 (1995)] and transport [S. H. Chun *et al* Physica **B284-288** 1442 (2000)] data suggest that the effective carrier number decreases with  $T$  increasing toward  $T_C$ .
  - [3] J. W. Lynn *et al*, Phys. Rev. Lett. **76**, 4046 (1996); J. A. Fernandez-Baca *et al*, Phys. Rev. Lett. **80**, 4012 (1998); J. Zhang *et al*, J. Phys.: Condens. Matter **19**, 315204 (2007).
  - [4] E. L. Nagaev, Phys. Rep. **346** 388 (2001).
  - [5] S. E. Lofland *et al*, Phys. Rev. **B56**, 13705 (1997).
  - [6] A. Moreo, S. Yunoki, and E. Dagotto, Science **283**, 2034 (1999); M. Uehara *et al*, Nature **399**, 560 (1999).
  - [7] E. Dagotto, T. Hotta, and A. Moreo, Phys. Rep. **344**, 1 (2001).
  - [8] T. V. Ramakrishnan *et al*, Phys. Rev. Lett. **92**, 157203 (2004); T. V. Ramakrishnan, J. Phys.: Condens. Matter **19**, 125211 (2007).
  - [9] M. Jaime *et al*, Phys. Rev. **B60**, 1028 (1999).
  - [10] A. J. Millis, R. Mueller, and B. I. Shraiman, Phys. Rev. **B54**, 5405 (1996).
  - [11] P.-G. de Gennes, Phys. Rev. **118**, 141 (1960).
  - [12] Unless the electron is localised on a single lattice site, the localised carriers also contribute to double exchange ferromagnetism. This effect is however weaker than for the itinerant electrons.
  - [13] See, *e.g.*, V. Chechersky *et al*, Phys. Rev. **B62**, 5316 (2000); F. Goya *et al*, J. Appl. Phys. **91** 7932 (2002).
  - [14] V. Chechersky *et al*, Low Temp. Phys. **23**, 549 (1997).
  - [15] E. Assaridis *et al*, Phys. Rev. **B75**, 224412 (2007).
  - [16] Other local magnetic probes, such as muon scattering [R. H. Heffner *et al*, Phys. Rev. Lett. **85**, 3285 (2000)] and nuclear magnetic resonance [G. Papavassiliou *et al*, Phys. Rev. Lett. **84**, 761 (2000)], also find several different contributions in the region around  $T_C$ .
  - [17] D.A.Shulyatev *et al*, J. Crystal Growth **237-239**, 810-814 (2002).
  - [18] S. B. Ogale *et al*, Phys. Rev. **B57**, 7841 (1998); J. Li *et al* J. Phys.: Condens. Matter. **16**, 2839 (2004).
  - [19] The resistivity of PSMO (Fig. 2, top) is indeed very close to that of PSMO-F; see also Table I.
  - [20] We defined  $T_C$  as a point where the derivative of the magnetic susceptibility,  $\partial \text{Re}\chi / \partial T$ , is minimal.
  - [21] P. Schiffer *et al*, Phys. Rev. Lett. **75**, 3336 (1995).
  - [22] M. B. Salamon and S. H. Chun, Phys. Rev. **B68**, 014411 (2003).
  - [23] C. P. Adams *et al*, Phys. Rev. **B70**, 134414 (2004); W. Li *et al*, J. Phys.: Condens. Matter. **16**, L109 (2004).
  - [24] We are aware of a sole exception [V. Chechersky *et al*, Phys. Rev. **B63**, 214401 (2001)], reporting emission Mössbauer data for a single crystal of  $\text{La}_{0.9}\text{Ca}_{0.1}\text{MnO}_3$ , which is well outside the metallic doping range.

- [25] I. Nowik and H. H. Wickman, Phys. Rev. Lett. **17**, 949 (1966).
- [26] J. M. De Teresa *et al*, Nature **386**, 256 (1997).
- [27] We note that in Ref. [9], the “magnetisation kinks” were attributed to the appearance of metallic islands (our  $T_2$ ).